Time transfer with nanosecond accuracy for the realization of International Atomic Time

D. Piester[1], A. Bauch[1], L. Breakiron[2], D. Matsakis[2], B. Blanzano[3], O. Koudelka[3]

[1]Physikalisch-Technische Bundesanstalt (PTB), Braunschweig, Germany

[2]United States Naval Observatory (USNO), Washington, DC, USA

[3]Technical University Graz (TUG) and Joanneum Research GmbH, Austria

1. Abstract

Two-way satellite time and frequency transfer (TWSTFT) has become an important technical component in the process of the realization of International Atomic Time. To employ the full potential of the technique, especially for true time transfer, a dedicated calibration is necessary. This consists of the calibration either of the operational link at large, including every component involved, or of the involved ground stations' internal delays only. Both modes were successfully employed by circulating and operating a portable reference station between the sites involved. In this article, we summarize the theoretical background for the different calibration modes applied and report examples of results from the 13 calibration campaigns performed up to now in Europe and between Europe and the United States. In all of these exercises, estimated uncertainties around 1 ns were achieved. Consecutive campaigns showed a very good reproducibility at the nanosecond level. Additionally, we address and briefly discuss sources that possibly limit the uncertainty for true time transfer employing TWSTFT.

Keywords: two-way satellite time and frequency transfer, TWSTFT, TWSTT, calibration, International Atomic Time, TAI, geostationary satellite, GEO

Acronyms used in this paper

CAL(i, k)	Calibration value, which has to be added to the raw TWSTFT measurement result between stations i, k to yield the true time difference between the clocks at stations i and k.
CCD(i, k)	Common-clock difference, TWSTFT measurement result between two TWSTFT setups (i, k) at one site, connected to the same clock
DLD(i)	Difference of signal propagation delay through the transmit and receive path of station i, TX(i) – RX(i)
EDV	Earth station delay variation, used to report known changes in the setup of a TWSTFT ground station
GEO	Geostationary satellite
PS	Portable Station, short form for a transportable TWSTFT ground station used in calibration experiments
RDY	Reference delay, time difference between the local time scale and the modem 1pps output synchronous with its TX signal
RX(i)	Signal delay in the receive path of TWSTFT station i
SCD(i)	Sagnac delay for a signal propagating from the GEO satellite to station i
SCU(i)	Sagnac delay for a signal propagating from station i to the GEO satellite
SP(i)	Complete signal path delay from station i to station k through the

	GEO, SPU(k)+SPT(k)+SPD(i)
TIC	Time-interval counter
TW(i)	Counter reading in the TWSTFT station i
TX(i)	Signal delay in the transmit path of the TWSTFT station i

2. Introduction

Two-way satellite time and frequency transfer (TWSTFT) [1] has been developed into a widely used technique of time and frequency transfer between laboratories that contribute, with their atomic clocks and, in some cases, with their primary frequency standards, to the realization of International Atomic Time (Temps Atomique International, TAI) [2]. The TWSTFT technique is, thus, used in two areas: for true time transfer, by comparing the phase differences between local realizations of the Coordinated Universal Time, UTC(*i*) in laboratories *i,* and for accurate frequency comparisons between atomic fountain clocks and hydrogen masers. At present, TWSTFT is performed operationally in at least two laboratories in the United States, twelve in Europe, and seven in the Asia Pacific Rim region.

It has already been reported that, in its present operational status, TWSTFT has the potential to enable time transfer down to the 1-ns regime and frequency comparisons at the 10^{-15} level for reasonable averaging times [3]. A further improvement down to stabilities of 10 ps in terms of time deviation should in principle be possible [4], but would require an overall delay stability of the link configuration (including ground stations and satellite) at the same level, which has not been yet achieved. Recently, frequency comparisons at the 10^{-15} level with an averaging time of 1 day were demonstrated by comparing hydrogen masers in remote European and U.S.

laboratories [5]. Another result of this study was that frequency comparisons based on GPS carrier-phase observables have the same or even a slightly better performance than TWSTFT. The accuracy for the determination of time scale differences via GPS, however, is rated at the 5-ns level, based largely upon a statistical uncertainty of 3 ns (root mean square) of repeated calibrations of individual operational receivers, some of which are observed to display ns-level jumps [6]. Such a value is typically reported in the BIPM *Circular T* [7] as the type-B uncertainty for GPS links, irrespective of the detailed type of GPS data and data processing used [8]. Here, TWSTFT has the ability for a considerably lower uncertainty. This was demonstrated for the first time by the calibration of three European TWSTFT ground stations using a portable station (PS) operated in parallel with them in 1998 [9].

At the time of this writing, nine TWSTFT links are used in the realization of TAI by the BIPM [7] connecting the Istituto Nazionale di Ricerca Metrologica (INRIM) in Torino, Italy, the Federal Office of Metrology (METAS) in Bern-Wabern, Switzerland, the National Institute of Information and Communcations Technology (NICT) in Tokyo, Japan, the National Institute of Standards and Technology (NIST) in Boulder, Colorado, USA, the Laboratoire National de Métrologie et d'Essais-Observatoire de Paris (OP), France, the Real Instituto y Observatorio de la Armada (ROA), San Fernando, Spain, the Swedish National Testing and Research Institute (SP) in Borås, the U.S. Naval Observatory (USNO) in Washington, DC, and the NMi Van Swinden Laboratorium B.V. (VSL) in Delft, the Netherlands, with the Physikalisch-Technische Bundesanstalt (PTB) in Braunschweig, Germany. These links are part of the "TAI-network" which connects about 60 timing centers world-wide. GPS time transfer is used on all other links [2]. Six of these so-called TAI-links were calibrated by means of TWSTFT. In this report, we give an overview on the calibration and recalibration of

several of these TWSTFT links and estimate the uncertainties achieved. We present an excerpt of the results that have already been described in conference proceedings as an illustration of what is possible with existing equipment. We also point out phenomena which are not well understood at present and which probably limit the achievable accuracy. Calibrations of links in the Asia Pacific Rim region were performed by NICT, but are not the subject of this paper [10].

A remarkable series of calibration exercises of the link between USNO and PTB was started in 2002 [11], as a part of the calibration activities of USNO [12,13,14,15]. The last exercise took part in November 2007. During the last few years, several European TWSTFT links, namely these between INRIM, METAS, NPL, OP, PTB, SP, the Technical University of Graz (TUG) in Austria, and VSL, were calibrated by means of TWSTFT employing the portable station of TUG [16,17,18,19] . The link calibration campaigns carried out up to now are listed in Table 1. The techniques applied differ between the USNO and the European practice, and this is described in the following section, where the necessary theoretical background for understanding the calibration practice is developed. Thereafter, the calibrations are described in Section 4. We discuss the results, including an uncertainty budget evaluation, in Section 5, and a comparison of consecutive campaigns is given in Section 6. An intercomparison between the USNO and European practice is described in Section 7. We conclude with a brief outlook and the acknowledgment for the many colleagues involved in the participating laboratories who helped during the campaigns and data computation.

Table 1: History of European (E1 to E5) and Transatlantic (T1 to T8) TWSTFT Calibration trips using the portable stations of TUG and USNO, respectively. For

laboratory acronyms, see the text. The Deutsche Telekom AG (DTAG) in Darmstadt, Germany, meanwhile stopped operation of their TWSTFT station.

No.	Year	Participating Institutes	Reference
E1	1997	TUG, DTAG, PTB	[9]
T1	2002	USNO, PTB	[11]
T2	2003	USNO, PTB	[13]
E2	2003	IEN, PTB	[16]
E3	2004	PTB, VSL, OP, NPL	[17]
T3	2004	USNO, PTB	[14]
T4	2004	USNO, PTB	[14]
T5	2005	USNO, PTB	[14]
E4	2005	PTB, SP, VSL, NPL, OP, INRIM	[18]
T6	2006	USNO, PTB	[15]
E5	2006	TUG, PTB, METAS	[19]
T7	2007	USNO, PTB	-
T8	2007	USNO, PTB	-

3. Theory

In this section, we recall the theoretical background and derive the equations necessary for a determination of calibration constants. We follow, if possible and expedient, the description and naming of the ITU-R Recommendation TF.1153-2 [20] and extend or deviate therefrom only if necessary. In particular, we will use some of the common abbreviating acronyms in the text and in equations, which are listed at the beginning of the paper.

TWSTFT between two remote stations 1 and 2 maintaining time scales UTC(1) and UTC(2), respectively, is based on two combined coincident measurements at both stations. Each measurement represents the determination of the time of arrival of a radio signal that is phase coherent to the remote atomic time scale and transmitted from the remote station with respect to the local time scale. The measurement result obtained at one site, e.g. TW(1), is the time difference reading from a time-interval counter (TIC). It comprises the difference between the two time scales, UTC(1)-UTC(2), and also the complete delay along the signal path. For the ground station, we distinguish only between the transmission (TX) and receiving (RX) part. The reader may find a more detailed description of the ground stations' components in Refs. [1,3,20]. We use Figure 1 to describe the individual signal delay components, e. g., for the signal received at site 1. The signal delay consists of the remote site transmitter delay TX(2), the overall signal path delay to the satellite and back to site 1 on Earth SP(2) (sum of the uplink delay SPU(2), the transponder delay SPT(2), and the downlink delay SPD(1)), the local receiver delay RX(1), and the delay due to the Sagnac effect [21], which is computed from the positions of the ground stations and the geostationary satellite (for an illustration, see [22]). We account for the Sagnac effect according to Ref. [20] by introducing Sagnac corrections for both the uplink and downlink to and from the satellite, SCU(2) = -SCD(2) and SCD(1) = -SCU(1), respectively. At site 2, the equivalent measurement is carried out simultaneously, and we obtain two measurement results, TW(1) and TW(2):

(1) TW(1)=UTC(1)-UTC(2)+TX(2)+SP(2)+RX(1)+SCD(1)-SCD(2)

(2) TW(2)=UTC(2)-UTC(1)+TX(1)+SP(1) +RX(2)+SCD(2)-SCD(1).

We assume at this stage a complete reciprocity of the signal path: SP(1) = SP(2). As mentioned above, the signal path consists of three components, SPU, SPT, and SPD. The satellite transponder delay cancels only if both ground stations transmit via a single transponder on the satellite, which requires that both stations are within the same antenna footprint of the satellite. This “ideal” transponder configuration is available for the European laboratories and on the X-band link between USNO and PTB, to be described later, but not in long-baseline links like the Ku-band links between Europe and the U.S. and between Europe and Asia. Here two transponders are used for the two directions through the satellite, and the propagation delays through the satellite equipment cannot be assumed to be equal. A calibration as described in this article is not possible as long as the difference of the transponder delays SPT(1)-SPT(2) is not known, which is normally the case. Furthermore, there are other effects causing non-reciprocities, resulting in SP(1)≠SP(2). However, most of these effects are small compared with the estimated calibration uncertainty. They will be discussed in Section 5.

The timescale difference can be computed by subtraction of (2) from (1):

(3) UTC(1)-UTC(2)=1/2[TW(1)-TW(2)]

+{1/2[DLD(1)-DLD(2)]+[SCD(2)-SCD(1)]}.

Here, DLD(i) is the signal-delay difference between the transmitter and the receiver part of station i, DLD(i) = TX(i) - RX(i). These delays are hard to determine

individually. Up to now, it has not been verified that they can be determined with nanosecond accuracy. Nevertheless, the development of station characterization devices is still in progress, and, thus, this problem may be solved in the near future [23,24].

Now we define the calibration value for the link between sites 1 and 2, which contains the terms in curly brackets in eq. (3):

(4) $CAL(1,2)= +1/2[DLD(1)-DLD(2)]+[SCD(2)-SCD(1)]$.

For its determination, two different approaches were applied. Their principles are discussed in the following paragraphs.

3.1. Calibration of a time transfer link – the "LINK" method

A simple way to determine CAL(1,2), designated LINK as introduced in [25], is to perform TWSTFT, providing TW(1)-TW(2), and using an independent time transfer link to provide UTC(1)-UTC(2). According to (3) and (4), a calibration constant can then be calculated from:

(5) $CAL(1,2)= [UTC(1)-UTC(2)]_{LINK}-1/2[TW(1)-TW(2)]$.

The independent time transfer results typically have been derived from GPS time transfer, despite of the fact that the uncertainty of GPS calibrations is inferior to TWSTFT-based calibrations. Among the TAI links today, the ones from NICT and NIST to PTB require this type of calibration.

In the TAI network, only the link between USNO and PTB has up to now been calibrated by TWSTFT in the LINK mode. Among the multiple techniques used on this link, one includes a geostationary satellite with up- and downlink frequencies in the X-band. The satellite antenna footprint extends from the U.S. East Coast to middle Europe and thus only a single transponder is needed. In the following, the USNO calibration method is described, which includes the use of a calibrated portable TWSTFT station (PS), additionally to the permanent ground stations. First, the PS is operated in parallel to station 1 connected to a common clock. Equation (3) is, thus, simplified to:

$$0=1/2[TW(1)-TW(PS)] + 1/2[DLD(1)-DLD(PS)]. \quad (6)$$

We define the common-clock difference CCD(1,PS) as -1/2[DLD(1)-DLD(PS)], and determine it from a TWSTFT measurement between 1 and PS as

$$CCD(1,PS)= 1/2[TW(1)-TW(PS)]. \quad (7)$$

Thereafter, the PS is transported to station 2 and connected with the corresponding time scale UTC(2). The time-scale difference UTC(1)-UTC(2) can be measured by performing a TWSTFT measurement between the PS located at station 2 and site 1; combining (3) with (7):

$$[UTC(1)-UTC(2)]_{LINK}=1/2[TW(1)-TW(PS@2)] -CCD(1,PS)+[SCD(2)-SCD(1)]. \quad (8)$$

SCD(2) and SCD(1) have to be determined separately from the exact positions of the stations and the satellite (see [20] and Section 5).

If the TWSTFT link to be calibrated is operated at the same time, the calibration constant can be computed according to (5). In addition, other time transfer links operated between the two sites can be calibrated in a similar way. The procedure is illustrated in Figure 2. Note that the TWSTFT link connecting regularly the two stations is not necessarily established through the same satellite that is used in the calibration.

3.2. Calibration of ground stations – the "SITE" method

Another possibility of performing a calibration includes the repetition of the CCD measurement described by (7) at a second and following sites. This will give further common-clock difference values, e.g. at site 2:

(9) $CCD(2,PS) = 1/2[TW(2)-TW(PS)]$

Forming (9) – (7) gives:

(10) $$CCD(2,PS)-CCD(1,PS)=1/2[DLD(1)-DLD(PS)]-1/2[DLD(2)-DLD(PS)]$$
$$= 1/2[DLD(1)-DLD(2)]$$

By using eq. (10), a calibration value according to eq. (4) can be computed. Because the nature of the measurement is a relative delay difference determination between

the PS and the stations to be calibrated at different sites, this method is called SITE [25]. Note that the calibration has a different characteristic compared to the LINK calibration. It is the determination of station delays, not a calibration of the end-to-end time transfer link. The requirements concerning the satellite transponder configuration, however, are the same as for the LINK mode. In Figure 3, the principle of the SITE mode is depicted.

3.3. Reporting Results

The equations to compute the calibration values for both methods LINK and SITE are:

(11) $CAL_{LINK}(1,2)= [UTC(1)-UTC(2)]_{LINK} -1/2[TW(1)-TW(2)]$ and

(12) $CAL_{SITE}(1,2)= CCD(2,PS)-CCD(1,PS)+[SCD(2)-SCD(1)]$,

respectively. Once a new CAL(1,2) has been determined, it should be reported in the corresponding data files according to [20]. In the file header, the following entries are reported: calibration identifier, type (“travelling station” for LINK mode calibrations and “portable earth station used in a relative mode” for SITE ones), Modified Julian Date (MJD) of the calibration (usually the first day at site 2), and an estimated uncertainty of the calibration. The determination of the latter will be discussed in the last section of this article. The calibration values are reported in the data lines in three distinct columns: the calibration identifier (referred to the header entry), the calibration switch (here only the case “1” is discussed; see [20] for details), and the calibration result. The calibration value is reported by the two sites with opposite sign. The value for station 2 is CAL(2,1) = - CAL(1,2).

Two additional quantities, the reference delay (RDY) and the earth station delay variation (EDV), have been introduced to document and report the result of time scale comparisons [20]. RDY reflects the difference between the ground station clock that synchronizes the TX signal and the local time scale, which is a constant value if the time scale is derived from the same clock. EDV reflects internal delay changes of the station due to changes in cabling or equipment since the last calibration. If a new calibration result is applied, this value is set to zero: EDV(1)=EDV(2)=0. In a particular ground station, the EDV values can differ from link to link, depending on the time of link calibrations and the time of setup changes. Finally, the timescale difference can be computed according to

$$\begin{aligned}(13)\quad UTC(1)-UTC(2) = {} & 1/2[TW(1)-EDV(1)]+RDY(1) \\ & -1/2[TW(2)-EDV(2)]-RDY(2) \\ & +CAL(1,2).\end{aligned}$$

4. Calibration of operational TWSTFT links in the European TAI network

Different standards of hardware and data acquisition are in use in the TWSTFT networks in operation today. The Asia-Pacific TWSTFT network [10,26] relies in particular on a different modem technology, which is currently incompatible with that in use in the European-USA network. The sites in Europe and the USA are being connected through the geostationary satellite IS 707 at 307° E, with transmit and receive frequencies in the Ku-band. On three transponders, 3.5 MHz bandwidth each have been contractually leased. One transponder covers Europe with both the up- and downlink beam. The frequencies are 14.0132 GHz and 12.5182 GHz,

respectively. As mentioned above, this transponder configuration is mandatory for a TWSTFT calibration, which is, thus, not possible in the transatlantic connection, where two transponders are being used. The one from USA to Europe (Europe to USA) is currently operated at 14.21175 GHz (14.21175 GHz) and 12.71675 GHz (11.91675 GHz), respectively. All stations use MITREX [27] and/or SATRE [28] modems, which provide fully compatible PRN signals. Each data point TW(*i*) in eq. (1) and eq. (2) is derived in the following way: Nominally 120 time-of-arrival measurements are made, one per second. At the end of the data collection, a second-order polynomial is fitted to the data and the nominal midpoint of the fit function represents the measurement value. It is exchanged between the institutes via the Internet in data files according to [19]. The measurement schedule and operational practices, including calibration campaigns, is coordinated by the CCTF Working Group on TWSTFT.

A calibration campaign starts at one site where the CCD is determined initially. Then, after transportation to a second site, the calibration measurements are carried out according to the SITE or LINK mode. After this experiment, additional sites can be visited. We start the description of the calibration procedure with the SITE mode, which was employed in European calibration campaigns (Section 4.1 to 4.3). Thereafter, the different practice of the LINK mode is described on the basis of USNO-PTB calibrations (see Section 4.4). In each case, the stability of the PS during the whole trip is crucial in the evaluation of the uncertainty of the calibration parameter. To verify the stability, it is common practice to start and end the calibration campaign at the same site. Ideally, the same result should be obtained in both experiments. In this section, the results for the three steps of a calibration campaign are described. We start with the initial CCD measurements, report on

typical measurement results as an input for the calibration constant calculation, and discuss the results of closure measurements and their impact on the uncertainty budget.

4.1. CCD

To give an example, in Figure 4 the results of the CCD measurements of the TUG PS at PTB during trip No. E4 are shown. On the left, the initial measurements and, on the right, the closure measurements are shown. The mean of the single measurements as well as the standard deviation of the single measurements around the mean (SD) are displayed. Sometimes the distribution of the single measurements around the mean is not Gaussian, as one can see clearly from the right graph, where obvious phase shifts during the measurement duration proves that other noise types than simple measurement noise are dominant. Because of the existence of such shifts, the SD value is used for the uncertainty, instead of the standard deviation of the mean. Later on (Section 4.3), we discuss typical results of the CCD measurements and the interpretation of results of the initial and the closure measurements.

4.2. Results obtained during the campaign

After the initial determination of the CCD, the PS is operated at remote sites in sequence. This was done in the SITE mode during the European campaigns (E1 to E5). In principle, no link of the remote stations has to be operated in parallel. However, it is very helpful if the regular links are in operation at the time of the campaign to enable a quick check of the data quality on site. We discuss in the

following briefly the results of campaign E4. That campaign started with the CCD measurements at PTB (see Figure 4 left). Then the PS was operated subsequently at SP, VSL, NPL, OP, and INRIM and this series was concluded by a closure measurement at PTB (see Figure 4 right). In Figure 5, the CCD measurements together with the mean and SD values are shown. The standard deviations (SD) varied between 0.2 ns and 0.7 ns, which is a typical data scatter range also observed in the other European campaigns E2 – E3 [16,17]. We have currently no explanation why the pattern of the individual data is so different between sites, but it was found to be to some extent reproducible [16,17,18]. Only in the very first campaign (E1), SD values of 0.1 ns to 0.3 ns were achieved, but the number of samples was quite small (only two to six data points were averaged) [9]. Here with some probability environmental effects could come into play, and some considerations on that are given in Section 5.

4.3. Return-Trip Closure

The second determination of the CCD after the PS returned to the initially visited station gives an estimate how the internal delays of the PS may have changed during the trip (Figure 4 right). Usually, for the determination of the calibration value, both CCD values are averaged or interpolated (if the closure experiment is done much later than the other measurements). For the estimation of the CCD uncertainty, we distinguish two cases: the difference $|CCD_1 - CCD_2|$ is either smaller than the combined standard deviation $CSD=\sqrt{\{(SD_1)^2+(SD_2)^2\}}$ or larger. As a conservative approach, the uncertainty is estimated to the larger of both values, reflecting that the observed delay change of the travelling station could have happened at any time during the campaign. In Table 2, the estimated uncertainties (bold values) of the past

European calibration campaigns are listed. The uncertainties range from 0.2 ns to 0.7 ns and, thus, are in good agreement with the observed statistical uncertainty of the measurements at all sites.

Table 2: Uncertainty of the (in)stability of the PS for the European campaigns E1 – E5, in ns. The values in bold face were accepted as the CCD uncertainty values.

Campaign	CCD_1	SD_1	CCD_2	SD_2	$\lvert CCD_1 - CCD_2 \rvert$	CSD
E1	4.146	0.148	4.304	0.261	0.158	**0.300**
E2	-278.024	0.196	-277.547	0.335	**0.477**	0.388
E2	694.683	0.034	694.135	0.624	0.548	**0.625**
E3	7.400	0.183	7.011	0.282	**0.389**	0.336
E4	41.025	0.306	41.116	0.597	0.091	**0.671**
E5	-20.102	0.157	-20.103	0.111	0.001	**0.192**

4.4. LINK mode calibration

At present the link between USNO and PTB is the only link combining USA with Europe that provides time transfer uncertainties at the 1-ns level. PTB and USNO as well as the PS are equipped with new generation SATRE modems, which enable a transfer of data across the link channel and provide a “clock-offset” value once per second. Each clock-offset value recorded in station 1 combines the instantaneously measured local TW(1) and a prediction of the remote TW(2) value updated every 4 seconds. The mean difference between the two methods of measuring the clock offsets is typically less than 10 ps, with a standard deviation of about 100 ps. It is,

thus, irrelevant which data the BIPM takes for its calculation of TAI. A quasi-real-time product of the time transfer is, thus, available. While this is not particularly important in current operations, it may be valuable for synchronization of the two Galileo Precise Timing Facilities, and for measurement of the GPS Galileo Time Offset (GGTO), via USNO [29], without the need of internet-dependent data links.

In normal operation, 13 minutes of one-per-second clock offsets are collected and averaged. In measurements with the PS, only 5 minutes of clock-offset values were typically averaged. Up to now, the link was calibrated eight times (No. T1 to T8) since 2002.

After the CCD has initially been determined at USNO, the PS is shipped to PTB and the link between the PS and USNO is established again, in parallel with the existing time links between USNO and PTB to determine the different CAL values. During the calibration campaign T2, to give an example, three links were operated in parallel and data from each are shown in Figure 6: the regular operational TWSTFT link with frequencies in the Ku-band, the regular link with frequencies in the X-band, and the link established with the PS. A comparison of the regular links, which had been calibrated earlier in campaign T1, with the PS measurements gives the corrections to be applied to the calibration parameters. During T2, this was done by averaging the time transfer data recorded during one day when the PS was in operation. The resulting regular time transfer averages were subtracted from the PS average, giving the corrections to be applied to the regular time transfer data. The corrections for the data of both days are (0.28 ± 0.41) ns and (0.00 ± 0.48) ns for the regular Ku-band and the X-band link, respectively. This perfect agreement is a rather good example. We discuss later the reproducibility of calibration exercises. In later campaigns (T3

onwards), first the difference between the PS measurements and interpolated regular time transfer data were computed and, in a second step, the data were averaged. SD values between 0.17 ns and 0.43 ns were achieved [14,15]. Occasionally, the closure measurement was not performed after transatlantic calibration campaigns, and the uncertainty was estimated from the values obtained during previous exercises. This seems to be justified if an already calibrated link is calibrated again and the new calibration value differs only slightly within the estimated uncertainty, and because return-trip data have almost always been found to be consistent with pre-trip data

5. Uncertainty evaluation

The overall uncertainty of the calibration value is estimated from the model equation (11) for the LINK method and from eq. (12) for the SITE method using the following expression:

$$U = \sqrt{u_{A,1}^2 + u_{A,2}^2 + u_{B,1}^2 + u_{B,2}^2 + u_{B,3}^2}\,, \quad (14)$$

where $u_{A,1}$ reflects the statistical uncertainty of the determination of the CCD (see Section 4.1) and $u_{A,2}$ reflects the statistical uncertainty of the measurements at the remote stations. For the LINK method, this corresponds to the SD of the comparison of the two operational links in parallel (see Section 4.4) and, for the SITE mode, to the SD of the CCD values at the remote sites (see Section 4.2). Some measurement series (see Figure 4 and 5: PTB_2, INRIM, and to a lesser extent SP) showed significant drifts that may be attributed to instabilities in the distribution systems of the local frequency or the one-pulse-per-second (1pps) signal, or the local TWSTFT station being calibrated itself. Environmental effects could contribute as a large factor to the statistical uncertainty, and this is suggested by most of the plots in Figure 5.

The nonlinearity of thermal and humidity effects is well known. As an example, in Figure 7 a multi-day common-clock data series between an X-band PS and an operational station at USNO is depicted, showing that in this particular case diurnals were essentially present at all times, but more pronounced at lower temperatures. The data, however, do not rule out the possibility that the two units have large, but identical, dependences at the higher temperatures.

The systematic uncertainty $u_{B,1}$ represents the stability of the PS. A lower limit is derived, following Section 4.3, by a comparison of the initial CCD measurements with the closure determination of the CCD. Thus, it represents in a strict sense the combined stability of both the PS as well as the collocated ground station. An additional systematic uncertainty is due to the connection of the PS to the local UTC generation system ($u_{B,2}$). This requires a connection of a local 1pps signal to the PS, which is usually done in two steps. First, the delay of the chosen 1pps signal to the local UTC(i) generation is determined (both signals need not necessarily originate from the same source) with a TIC and the 1pps is then connected to the PS, where its rising edge triggers an internal TIC. $u_{B,2}$ is usually estimated based on the specifications of the TIC in use (0.5 ns). In $u_{B,3}$ all other suspected possible systematic effects are included. These effects are, e.g., the instability of the connection to the local UTC (0.1 ns), changes in TX/RX-power and C/N_0 during the campaign, and the use of different PRN codes compared with the operational modes (overall 0.1 ns to 0.2 ns). During the European campaigns, PTB always used a portable caesium clock to connect the PS to UTC(PTB). Thus, an additional 0.3 ns uncertainty was assumed for links where PTB is involved. The systematic variations seen in Figure 4, right, could also be caused by the instability of the used clock, whereas no such effect can be expected at all other sites.

The uncertainty estimation results so far achieved are summarized in Table 3. Note that during the LINK mode calibrations, the statistical uncertainty for the remote measurements is increased ($u_{A,1} < u_{A,2}$). This is probably due to the longer baselines compared with the effective zero baseline during the common-clock measurements and/or due to the fact that two time transfer links operated simultaneously contribute to the noise.

Table 3: Ranges of the uncertainty estimated for the SITE and LINK mode calibrations as reported for the aforementioned calibration exercises.

Method	$u_{A,1}$ (ns)	$u_{A,2}$ (ns)	$u_{B,1}$ (ns)	$u_{B,2}$ (ns)	$u_{B,3}$ (ns)	U (ns)
LINK	0.07–0.21	0.19–0.37	0.59–0.80	0.5	0.14	0.87–1.01
SITE	0.30–0.72	0.16–0.72	0.48–0.67	0.5	0.22–0.37	0.88–1.26

The overall estimated uncertainties were in all cases in the range 0.8 ns to 1.2 ns. More detailed information about the uncertainty estimations of the individual campaigns were reported in the corresponding conference reports. The reproducibility of consecutive calibration campaigns (see next section), even partly employing different operational modes, suggest that the estimations are well founded. However, the consistency of the calibrations does not rule out the existence of consistently unmodelled errors.

We add a few more words on further unaccounted contributions to the calibration uncertainty. In a regular TWSTFT network, the operational parameters should be kept as constant as possible. These are the TX frequency, the TX power, and the PRN code used. The influence of the transmitter power variation has been investigated [30,31], but the underlying effects are not completely understood at

present. Under normal conditions, a change of the TX frequency is not necessary for either routine operation or a calibration campaign; SITE-based calibrations would be invalidated by frequency differences more than a few MHz due to the frequency-dependence of the equipment. The TX-power levels of the participating stations of a calibration campaign should be kept in a range of ± 1 dB if possible. Whether this has been obeyed during all campaigns may be questioned. As mentioned above, the PRN codes used have to be changed during a calibration exercise in the SITE mode, and this may cause a non-negligible measurement uncertainty. A first investigation showed no significant difference in the calibration results employing different PRN codes [17]. A direct comparison of the SITE with the LINK method allows a further estimation. This is discussed in Section 7 in more detail.

In principle, the determination of the Sagnac correction contributes to the uncertainty budget. However, if the ground stations' positions are known with an accuracy of some tens of meters, the uncertainty remains below 1 ps. As a rule of thumb, one gets 1 ps per 30 m for European stations and a GEO at 307° E. The satellite movement around its center position on its geostationary orbit has a small influence on the time transfer measurements due to the satellite velocity [4] and its position [32], but in all normal cases, the effects remain below 0.1 ns.

Finally, it cannot be excluded that the transponders in the satellites used change their internal delays at the nanosecond level. The satellites rotate once a day as they follow the Earth, and thermal gradients within the satellite would be expected to follow the direction of the sun. In fact, diurnal periodical variations on the time transfer data sometimes show amplitudes of 2 ns [32,33], especially in the transcontinental links, where two different transponders are used. These diurnal variations are usually

less pronounced in the intra-European TWSTFT links, but the European stations also have a more common environment. Since USNO and NIST often show different diurnal patterns with the European sites, it is difficult to separate effects. Up to now, there is no clear model of how to account for these variations in the uncertainty evaluation. Use of daily mean values based upon many data points (12 at least) equally distributed over 1 day would average out any diurnal variations, but weekly and seasonal variations, whatever their cause, would remain as ns-level sources of uncertainty.

6. Reproducibility of TWSTFT calibrations

Up to now, eight TWSTFT calibration campaigns (T1-T8) of the USNO-to-PTB link have been completed by USNO. This allows a good assessment of the stability of each of the links, since they are each based on completely different ground and space equipment. The required differential corrections to the calibration values for the two TWSTFT links UTC(PTB) – UTC(USNO) as determined after each calibration exercise are displayed in Figure 8. Only small corrections were needed. For the Ku-band link (X-band link), the mean value of the corrections amounted to −0.46 ns (−0.50 ns) with SD of 1.43 ns (1.26 ns). The error bars represent the estimated measurement uncertainty at the day of the calibration. The gray bars reflect the estimated uncertainty of the time transfer link at the day of calibration, based on previous calibration results. After a recalibration, the uncertainty of the determination of the calibration value becomes the uncertainty of the time link itself. It is obvious that the estimated uncertainty can only be increased or remains the same between two calibration campaigns. Thus, the gray bars are always equal or larger than the

error bars of the former exercise. The exchange of components after operational failures has usually led us to increase our uncertainty estimates. In summer 2003, e.g., both links (Ku- and X-band) broke down at the same time for a period of several days. After the replacement of ground station components, the internal delays were changed. Dual-frequency, multi-channel common-view GPS time transfer was conducted all the times and allowed us to bridge the gap in the TWSTFT links so that the CAL values could be corrected, but at the price of a larger uncertainty. To demonstrate the stability of the links at the time of this writing, we show the double differences of USNO-PTB comparisons via the two TWSTFT links in Figure 9.

In the European TWSTFT network, only few TAI-links were calibrated a second time and there is no link which has been calibrated more than twice up to now. Omitting links where larger modifications in the setups were done in between the calibrations, the values of the most recent campaign (E4) differ only slightly from the previous values in the case of the links INRIM – PTB (-0.76 ns), NPL – PTB (-0.62 ns), and OP – PTB (-1.53 ns). The common sign of these results (mean = -0.97 ns) indicates a potential instability of PTB's ground station.

The values given above are in good agreement with the long-term stability of TWSTFT links when compared with other techniques operated in parallel. On the long-baseline link between the USA and Europe, peak-to-peak variations of about 2 ns are observed comparing TWSTFT with GPS carrier phase over months [34,35]. Even C/A-code single-frequency GPS receivers have shown excellent behaviour compared to TWSTFT in the link between PTB and NIST, as illustrated in Figure 10.

7. Comparison of the calibration methods

Under the presumption that the signal path delays and delays in all ground stations involved are the same during the calibration as well as in routine operation, the LINK and SITE techniques are equivalent. This implies that the signals from the PS are transmitted through the same GEO satellite as those exchanged in regular operations. As this has been the case in all European calibration exercises, the campaign E4 was used to test if the theoretically equivalent methods LINK and SITE give the same results by operating the PS at the remote sites in both modes. The CAL values were derived from the SITE mode, and the LINK mode data were used to investigate possible discrepancies between both methods. A comparison between both methods requires a sufficiently dense measurement schedule for links, the regular one and the one established with the PS. In Figure 11, a comparison of both methods for the link UTC(OP) – UTC(PTB) is displayed. The regularly operated Ku-band link between both laboratories (open dots) was adjusted afterwards with the results of the SITE mode calibration values. When the PS was in operation at OP, additional measurements in the LINK mode were performed (full dots). These direct time transfer measurements (see Figure 6) enable a comparison between both modes by subtracting LINK – SITE, the result of which is shown in Figure 12. For each data point of the LINK mode, the two chronologically adjacent data points of the SITE mode calibrated UTC(OP) – UTC(PTB) were interpolated and then subtracted from the LINK data. The mean value of less than 0.1 ns is insignificant with respect to the overall statistical uncertainty SD = 0.4 ns.. For a combined uncertainty, only systematic effects due to code changes or power variations (u_{B3}) have to be accounted for (0.1 ns). This is due to the fact that the other systematic (u_{B1}, u_{B2})

would cause the same offset in both methods. The total combined uncertainty is, thus, 0.42 ns, only a bit higher than the SD.

The comparison for the link OP- PTB gave the best results. In Table 4, the results for in total four TAI links calibrated during this campaign are listed. Except for the link between VSL and PTB, the mean differences lay within the estimated 1-σ uncertainty. The excess deviation may be explained by influences of out-of-range operational parameters such as TX power and/or corresponding RX C/N_0 values, which should be monitored more accurately during upcoming campaigns.The statistical uncertainty of the SITE mode calibration would be expected to be slightly lower than the statistical uncertainty of the LINK mode (see Section 3), because of fewer noisy signals are compared and because ionosphere, satellite position, and site position errors, each estimated to be <100 ps, cancel completely in the SITE Mode. More importantly, there will also be cancellation of thermal and humidity effects, to the extent that the equipment have identical dependencies. However, comparing the SD for both methods (see $u_{A,LINK}$ and $u_{A,2,SITE}$ in Table 4) shows no clear picture, which might also be due to the small data base for the LINK method. In general, one has to concede that many of the above statements could be made with better confidence if more data would have been collected. This would, however, have required a longer operation of the PS at each site and, thus, higher cost for each of the campaigns.

Table 4: Mean statistical and combined uncertainty of LINK – SITE for four links calibrated during campaign E4, evaluated as described in the text. Additionally, the SDs for the remote SITE measurements, as depicted by the error bars in Figure 8, are listed.

Link	Mean (ns)	samples	$u_{A,LINK}$ (ns)	U_{LINK} (ns)	$u_{A,2,SITE}$ (ns)
NPL-PTB	0.24	4	0.27	0.35	0.72
OP-PTB	0.01	16	0.35	0.42	0.57
SP-PTB	-0.55	6	0.57	0.61	0.29
VSL-PTB	-1.01	6	0.48	0.53	0.16

To conclude this section, we wish to answer the question whether LINK and SITE calibrations are equivalent in a more general sense. First, we take a look at the benefits of both techniques. Because both methods calibrate the time difference between the 1-pps on-time points at the two stations of a link, either can be used to calibrate any time transfer link between two visited sites. They are not limited to TWSTFT links. Also GNSS links (i.e. GPS, GLONASS, and the future Galileo) can be calibrated by means of TWSTFT. Calibrating GPS links by means of TWSTFT may be a favourable option to combine the advantages of both techniques, the accuracy of TWSTFT and the relatively low costs for operating a GPS receiver. A calibration of the time link between PTB and the Austrian metrology institute BEV (Bundesamt für Eich- und Vermessungswesen, Vienna) following this idea took place in mid October 2007.

The SITE technique can be used if for any reason both of the operational TWSTFT stations in the link to be calibrated cannot be operated with the PS's simultaneously available at the sites at the ends of the link. . Presuming that the internal delay of the PS is constant in between subsequent calibration campaigns, all CCD measurements

of these campaigns can be combined and links between all stations can finally be considered as calibrated even if they did not participate in the same campaign. A monitoring of the delay stability of the PS in between subsequent campaigns is mandatory to estimate the uncertainty of all the calibration values.

Both methods also have drawbacks. In the LINK method, three measurements are necessary for the determination of the calibration value, i.e. the PS at site 1 in a common-clock mode with station 1, the PS at site 2 doing TWSTFT with station 1, remotely, and the regular time transfer station 1 to station 2. Compared with the two CCD measurements required in the SITE method, this additional measurement will introduce additional noise. For each technique, the statistical noise of any step may be reduced by increasing its duration.

The two techniques also differ in their sensitivity to environmental effects. In addition to what was said in Section 5, here we note that all exterior TWSTFT stations do not have identical thermal dependences, nor necessarily do they have the same as the PS. To the extent they do have the same dependencies, the SITE technique will yield more internally consistent values.

A drawback of the SITE mode is that the stations' operational parameters during regular TWSTFT operations differ in details from those used during the calibration measurements with the PS. Some of these operational parameters may have an influence on the measurement results. The delay in the RX path of a station may be dependent on the signal structure of the received signal [36,37]. In fact, PRN codes have to be changed at least at the PS's modem (to receive the signals from the different visited stations). The impact was discussed in the uncertainty budget

evaluation (Section 5); actually it represents a systematic offset which is a property of the links, as opposed to one of the stations.

The so-called “multiplicative band-pass effect” can result in erroneous SITE-mode calibration values. It occurs because the signal delay is a function of the frequency and can vary over the (typically) 2-MHz widths of the band-pass filters in the modems. The actual spectral shape of the transmitted and received signals depends upon the spread-spectrum code and the frequency dependence of the delays of the individual stations multiplied together. Therefore the product of the contributions between a PS and each site is not the same as the product between those of the two sites. The net effect in our data has been estimated using regularly collected Ku-band data by computing so called three-cornered-hat round-trip closure sums between mutual observations of triplets of laboratories. If all site-based corrections are consistently applied, or not applied at all, then we expect:

(14) [TW(1)-TW(2)] + [TW(2)-TW(3)] + [TW(3)-TW(1)] = 0

Any deviation from zero would not be measurable by the SITE calibration, provided the same equipment was used by each laboratory for each observation. Previous studies, using an earlier generation of modems, reported effects as strong as 8 ns, as quantified by the expression in (14) [37]. Transatlantic Ku-band observations would not be expected to have zero round-trip closure, because slightly different transmission and reception frequencies are used for comparisons within Europe and across the Atlantic, respectively. In some stations, even different hardware components are used. Using publicly available Ku-band data, we have computed the closure sums for a large number of triplets involving the European stations over a 2-year period. So as to minimize the shorter-term effects of noise, clock variations between observations, and diurnal signatures, we have grouped the data into bins of

about 50 days, and calculated 50-day mean closure values. As an example, in Figure 13 the results of a subset of triplet closures involving PTB is depicted. In total, 720 such closure values were considered as significant in the present context and a histogram of their absolute values is shown in Figure 14. The 50-day averages typically display non-Gaussian behaviour, are not in general of zero mean, and their point-to-point scatter (first differences) is typically larger than the statistical errors expected from averages over up to 600 individual sessions (12 measurements per day, 50-day averages). All of these facts are consistent with the existence of variable link-based systematic effects whose magnitudes are, however, less than 1 ns on average for most of the links. But a systematic examination of the existing data has just begun and will be continued, and we note that one European station was excluded from the analysis because triplets including it often had closure sums of 3-4 ns.

8. Conclusion

In this paper, we have summarized the theoretical background and experimental experience of the calibration of TWSTFT links using a portable station, which started in 1997. We have shown that the established practice provides for the first time the possibility for time transfer with true 1-ns accuracy, which is used for TAI computation and other scientific applications.. From the experience of several calibration exercises, it is proved that this uncertainty level can be reliably reached in campaigns, as long as no operational failures occur. Consecutive calibration campaigns show that the reproducibility is at the same level as the estimated uncertainty if in the mean time the time links are operated continuously without major system changes and failures.

At present, the link instabilities including the ground stations, e.g. due to environmental influences, is at the nanosecond level, too. Thus, for keeping the accuracy within 1 ns, it is mandatory to calibrate the links on a regular basis. Other influences, e.g. transmission power or the use of different PRN codes, were investigated only briefly and are not clearly understood today. However, the possible influence is at the level of a tenth of a nanosecond for the former, but may be at the nanosecond level for the latter. For a further improvement of the TWSTFT technique, it seems to be advisable to study the stability aspects regarding the above-mentioned points in a next step.

9. Acknowledgments

Organization, execution, and evaluation of TWSTFT calibration campaigns are not possible without the substantial support of several individuals from all participating institutes. The authors would like to express their gratitude for the help of the various colleagues listed subsequently at many stages of the calibration campaigns reported in this paper: J. Achkar (OP), J. Becker (PTB), F. Cordara (INRIM), B. Fonville (USNO), J. Hirschauer (USNO), R. Hlaváč (formerly at NPL), K. Jaldehag (SP), G. de Jong (VSL), C. Karel (TUG), E. Kroon (VSL), L. Lorini (INRIM), A. McKinley (USNO), P. Merck (OP), T. Polewka (PTB), H. Ressler (TUG), M. Rost (PTB), C. Schlunegger (METAS), I. Sesia (INRIM), A. Smith (formerly at USNO), and P. Whibberley (NPL). The authors appreciate the technical support by W. Schäfer and A. Pawlitzki of Time Tech GmbH, Stuttgart, and invaluable advice by Bill Klepczynski, Head of the CCTF Working Group on TWSTFT. Until August 2006, the transponder on IS-707 was provided free of charge by the Intelsat General Corporation.

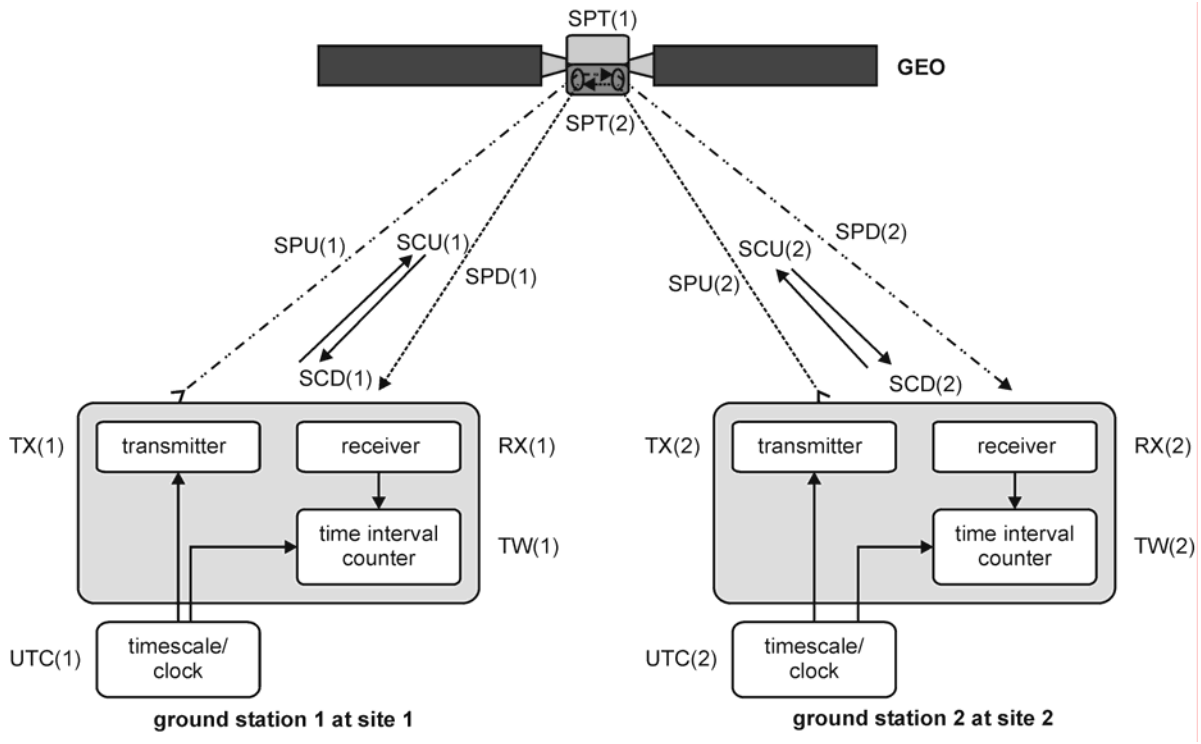

Figure 1: Setup and signal paths of two TWSTFT ground stations 1 and 2 operated at remote sites 1 and 2 maintaining time scales UTC(1) and UTC(2), respectively. For details, see the text.

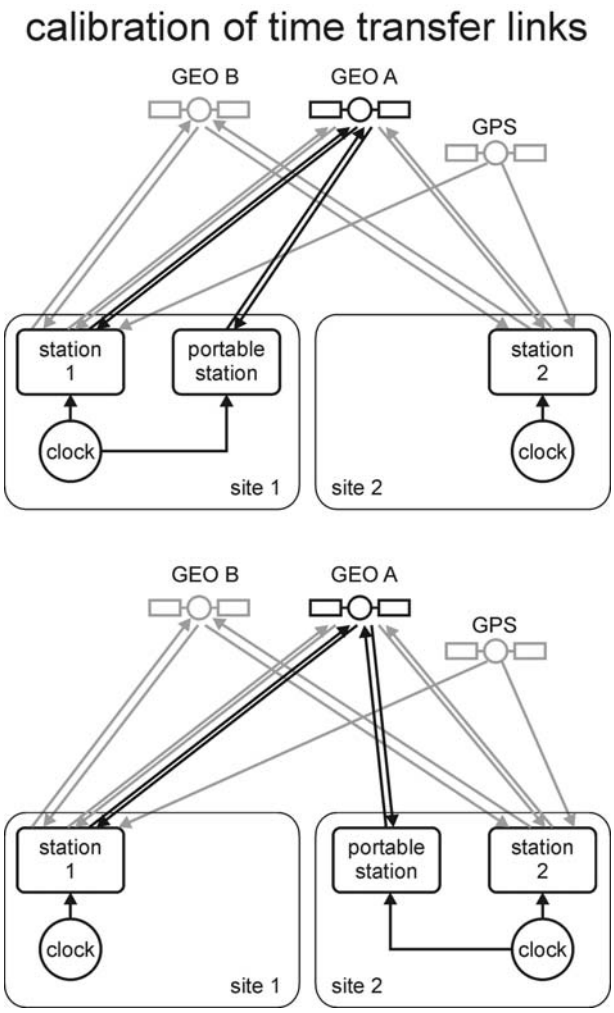

Figure 2: Two-step calibration of a time link. The portable station is operated at laboratory 1 in a common-clock mode with station 1 via GEO A (upper part) and then shipped to the remote laboratory 2, where the true time transfer measurement (typically again via GEO A using the same transponder configuration) is performed (lower part). Thereby, other links (e.g., via GEO A, via GEO B or via GPS) can be calibrated.

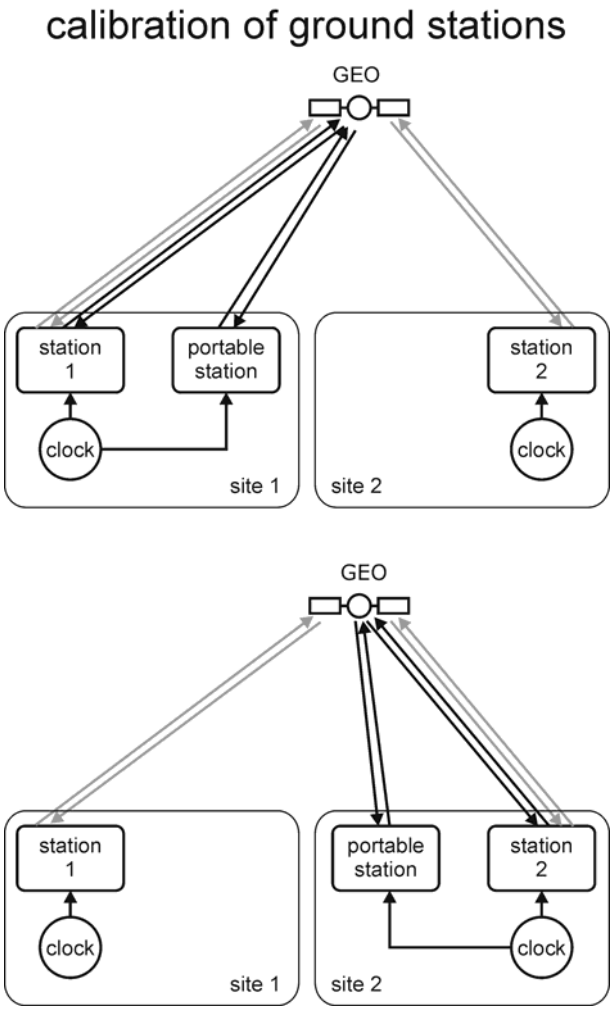

Figure 3: In the SITE mode, the delay difference between a portable station and a number of ground stations is determined in sequence. Here, we see how just two stations are calibrated by a portable station. Upper part: CCD(1,PS) is determined at station 1; lower part: CCD(2,PS) is determined at station 2.

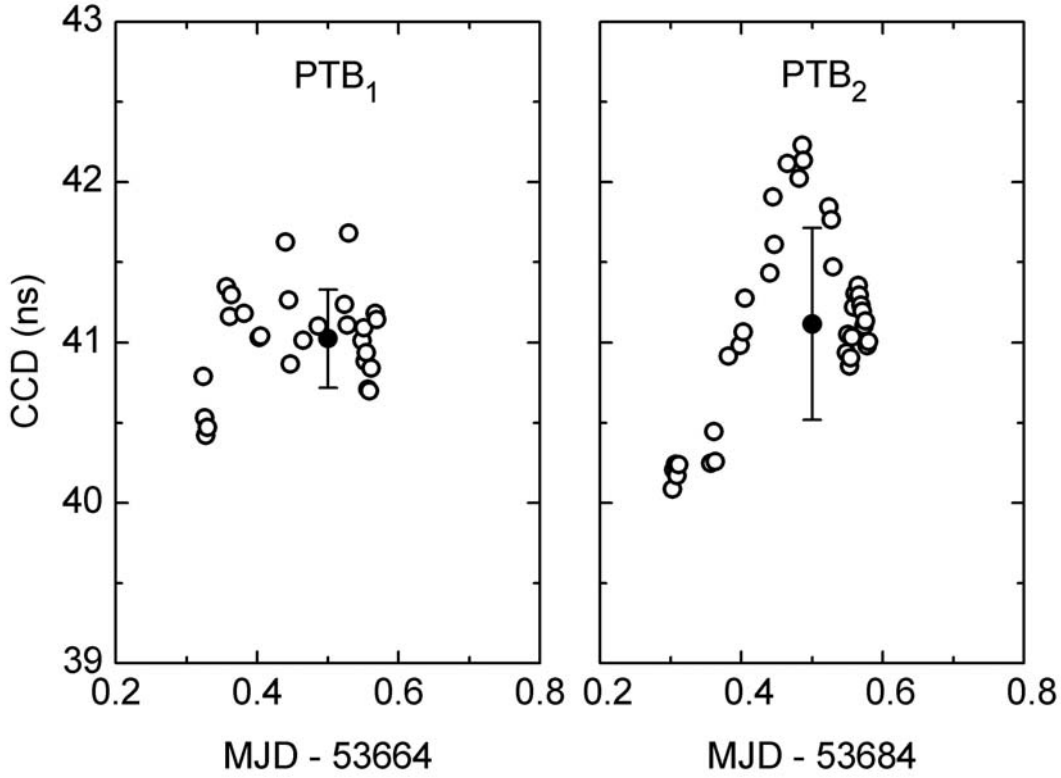

Figure 4: Individual CCD measurements (open dots), mean values (solid dots), and standard deviations (bars) of the single CCDs between the PS and the local station at the beginning (left) and the end (right) of calibration trip No. E4. MJD 53664 corresponds to 21 October 2005.

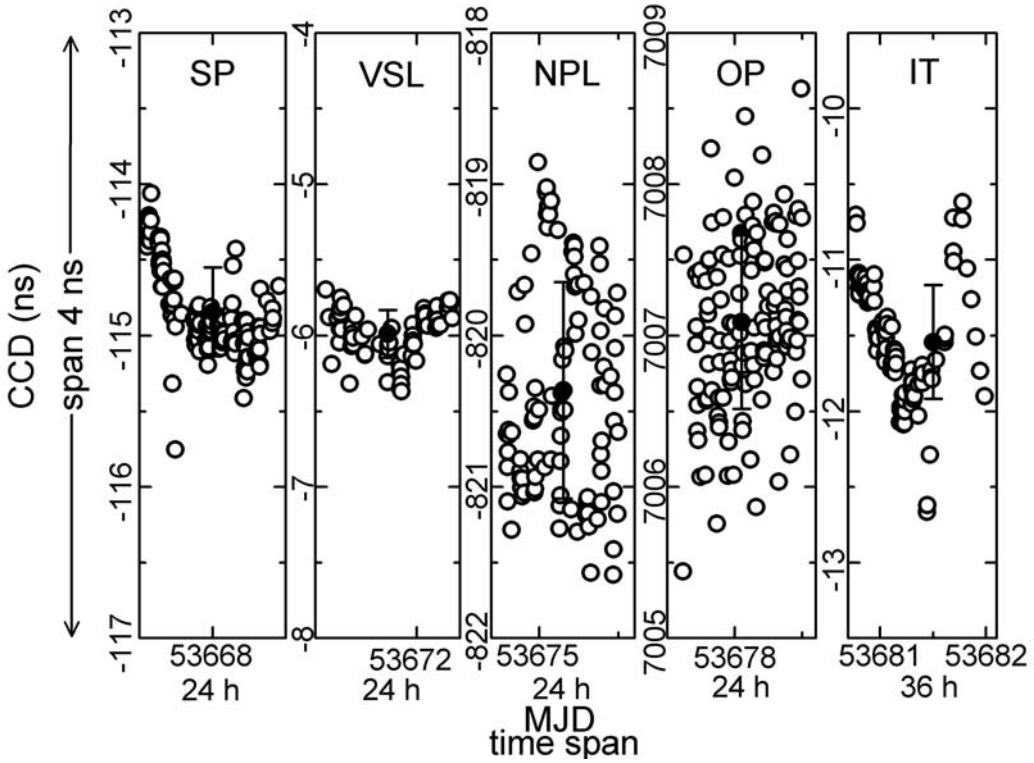

Figure 5: Individual CCD measurements (open dots), mean values (solid dots), and standard deviations (SD) of the single CCDs between the PS and the local station. IT is the short-form designation of INRIM.

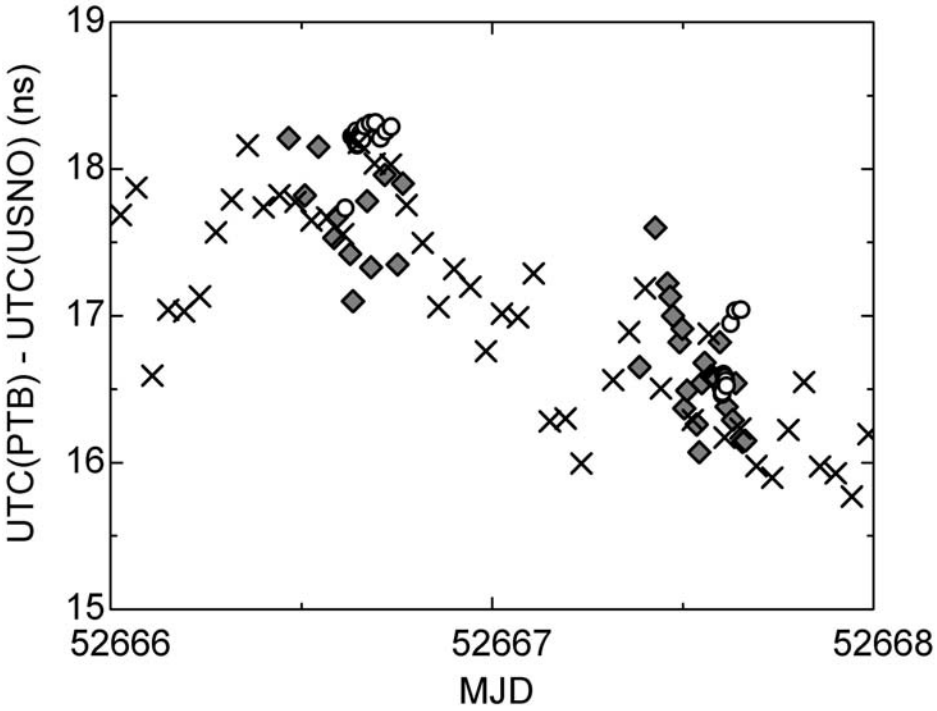

Figure 6: Time scale comparison UTC(PTB) – UTC(USNO) during calibration campaign T2 using Ku-band (open dots), X-band (crosses), and the X-band PS (gray diamonds). The link established with the PS was operational on 27 and 28 January 2003 (MJD 52666 and 52667). At that time the Ku-band link was operated only three times per week, each time for 1 hour. During the calibration campaign, extra sessions were arranged.

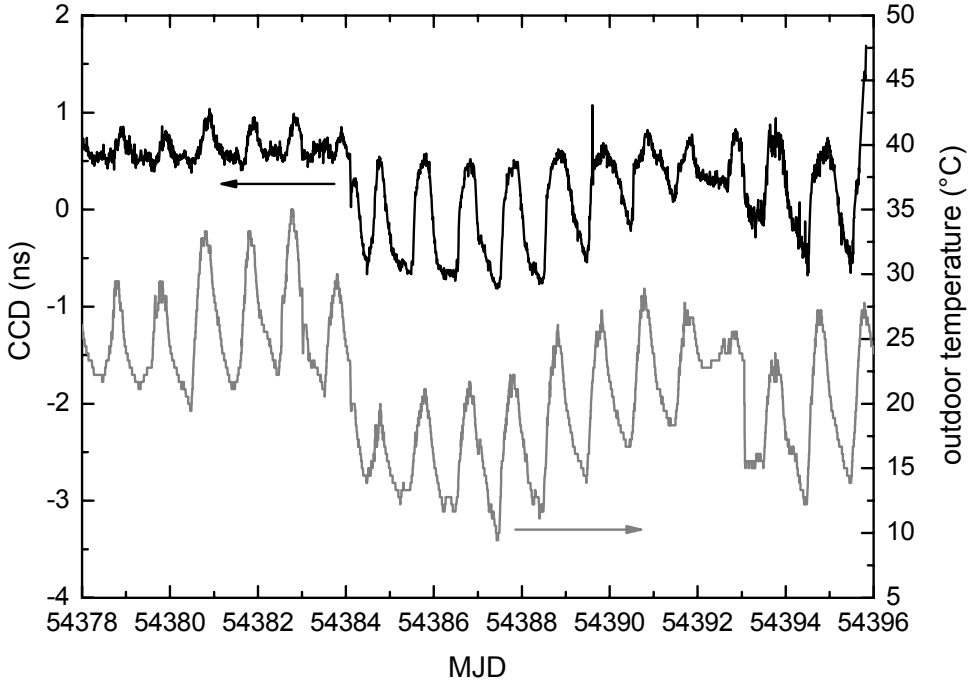

Figure 7: CCD between X band TWSTFT systems and exterior temperature at USNO, showing particularly large diurnal variations at lower temperature.

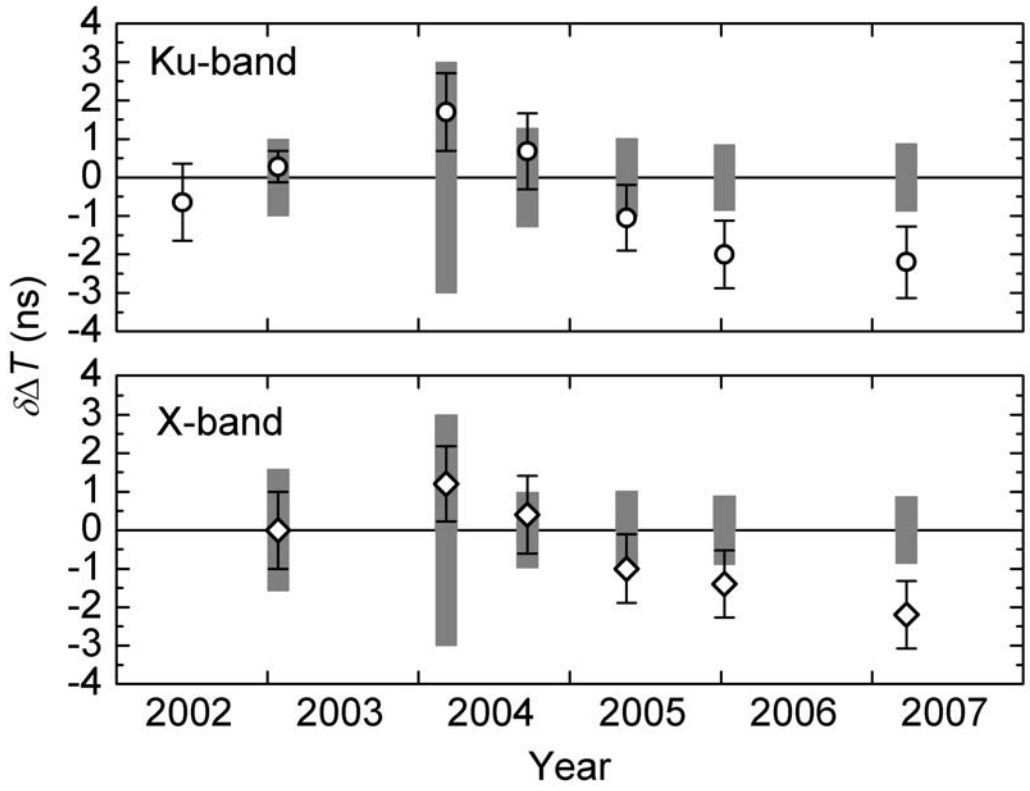

Figure 8: Time Offset “operational link minus PS” obtained for the routine TWSTFT links in the Ku-band (upper graph) and X-band (lower graph) in the comparison UTC(PTB) – UTC(USNO) and the associated uncertainty (error bars). The gray bars reflect the link uncertainty based on past calibrations. In 2002 and earlier, the Ku-band link was calibrated by using GPS results with an error bar exceeding the scale in the figure. The time offsets were subsequently applied as differential corrections to the calibration constants valid for each link.

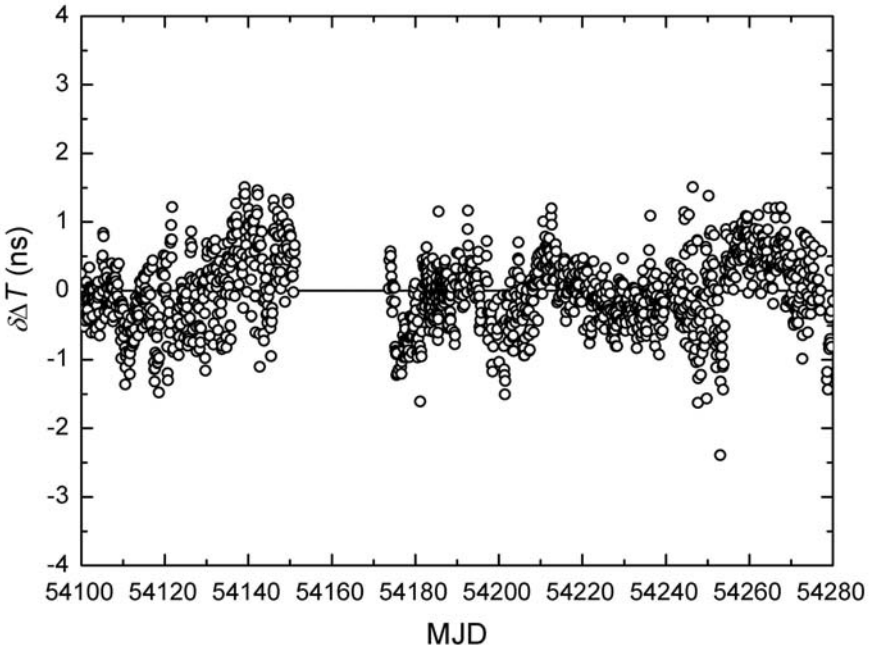

Figure 9: Double differences UTC(USNO) – UTC(PTB) via the two TWSTFT links (X-band minus Ku-band results) over 6 months (January to June, 2007), see also caption of Figure 10.

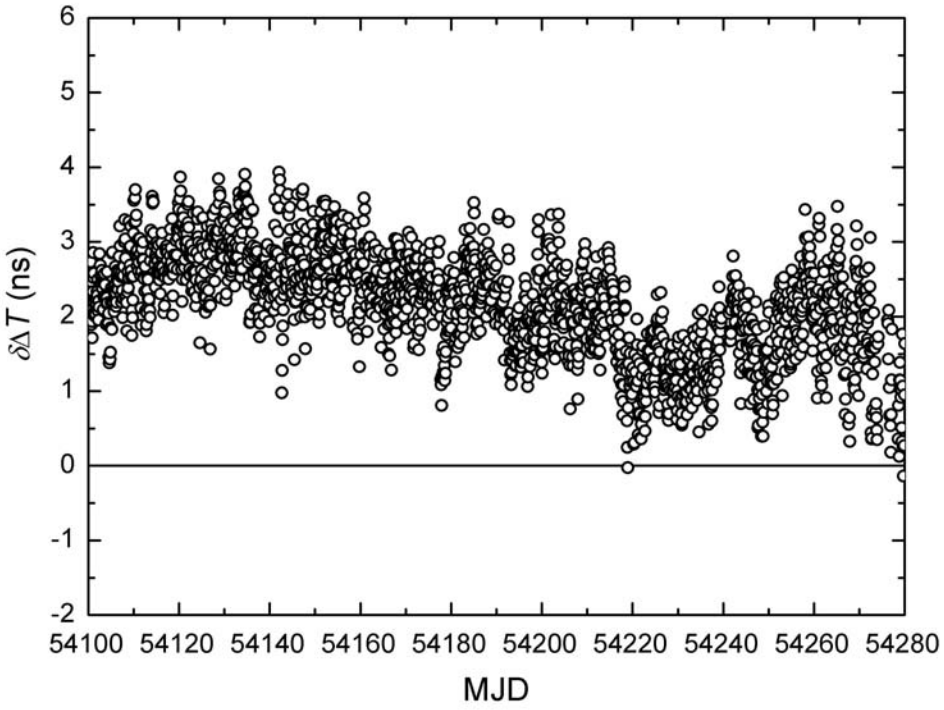

Figure 10: Double differences UTC(NIST) – UTC(PTB) via TWSTFT (Ku-band) and using GPS C/A code single-frequency receivers in both institutes over 6 months (January to June 2007). Data were retrieved from the BIPM ftp server [38] As explained in the "Readme" file on this site, GPS links are computed with data corrected for IGS precise ephemerides, solid Earth tides, and ionospheric delay from IGS maps. Vondrak smoothing is applied for suppressing measurement noise.

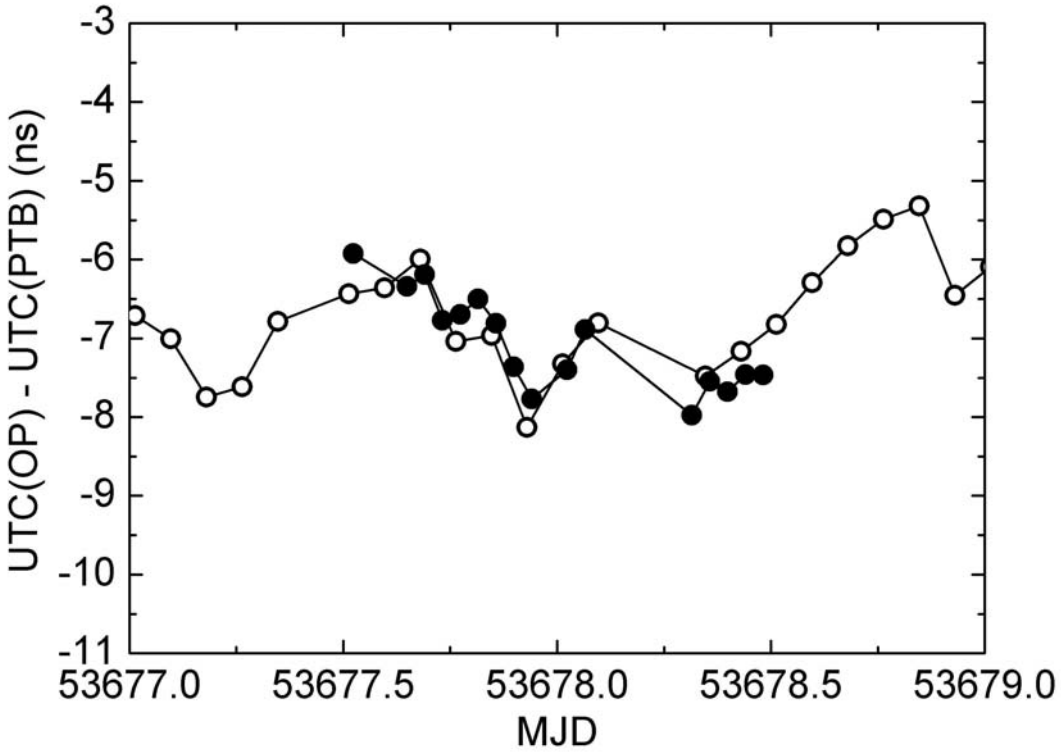

Figure 11: Comparison of the two calibration modes: time transfer data UTC(OP) – UTC(PTB) with the result of the SITE mode calibration (open dots) and the results of the LINK measurements (full dots) at the day of calibration at OP during campaign E4. MJD 53677 corresponds to 3 November 2005.

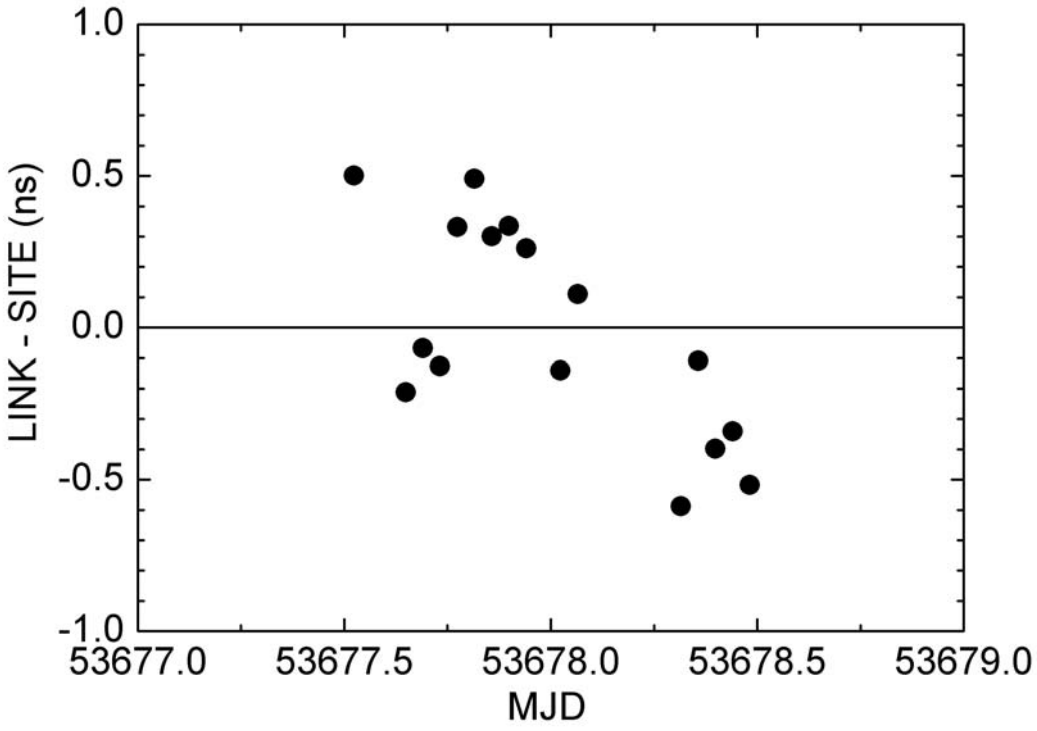

Figure 12: Difference LINK – SITE from Figure 11. For each data point of the LINK mode, the two nearest SITE-mode-calibrated UTC(OP) – UTC(PTB) data points were interpolated and then subtracted from the LINK data.

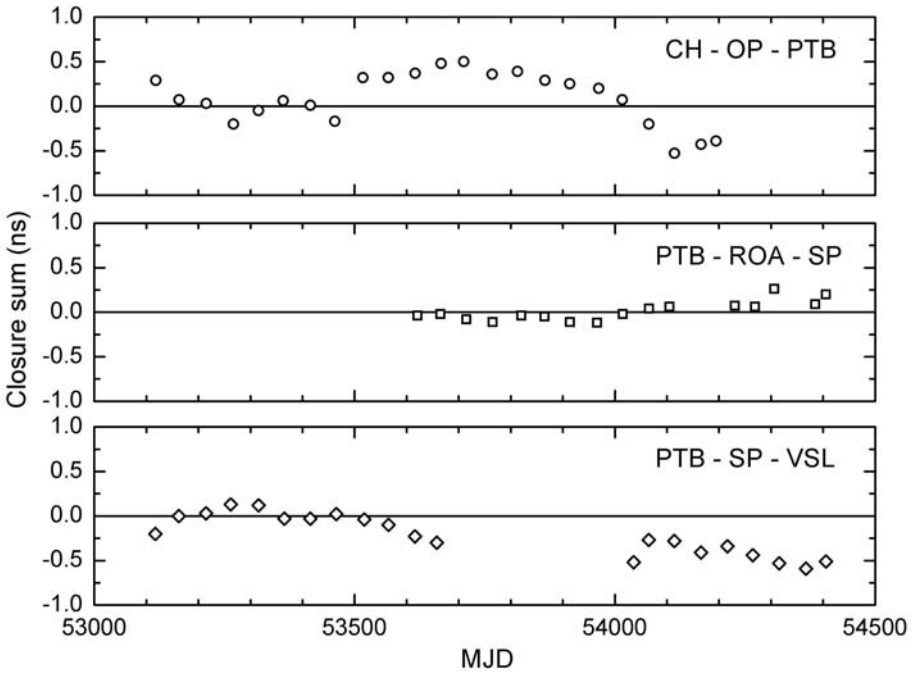

Figure13: Example of TWSTFT closure sums (14) for three links involving PTB. Each data point represents an average over all closures obtained during a 50-day interval.

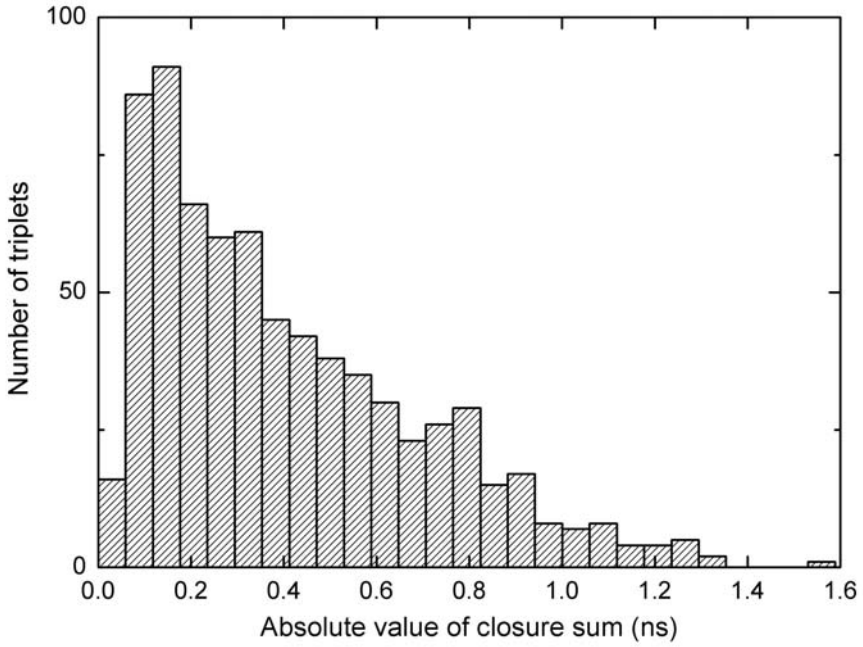

Figure14: Histogram of the absolute values of 50-day averages of closure sums of timing differences combining most European TWSTFT stations between MJD 52900 and 54400.

10. References

[1] Kirchner D 1991 Two-Way Time Transfer Via Communication Satellites *Proc. of the IEEE* **79** 983-989

[2] Guinot B and Arias E F 2005 Atomic time-keeping from 1955 to the present *Metrologia* **42** S20-S30

[3] Kirchner D 1999 Two-Way Satellite Time and Frequency Transfer (TWSTFT): Principle, Implementation, and Current Performance *Review of Radio Science 1996-1999* (Oxford: Oxford University Press) pp 27-44

[4] Parker T E and Zhang V 2005 Sources of Instabilities in Two-Way Satellite Time Transfer *Proc. 2005 Joint IEEE Int. Freq. Contr. Symp. and Precise Time and Time Inerval (PTTI) Systems & Applications Meetin*g *(Vancouver, Canada)* pp 745-751

[5] Bauch A, Achkar J, Bize S, Calonico D, Dach R, Hlaváč R, Lorini L, Parker T, Petit G, Piester D, Szymaniec K and Uhrich P 2006 Comparison between frequency standards in Europe and the US at the 10^{-15} uncertainty level *Metrologia* **43** 109-120

[6] Matsakis D, Lee M, Dach R, Hugentobler U and Jiang Z, 2006 GPS carrier phase analysis noise on the USNO-PTB baseline, *Proc.IEEE Int. Frequency Control Symposium and PDA Exhibition (Miami, FL, USA, 2006), pp 631 - 636*

[7] *Circular T*, a monthly publication of the BIPM (see http://www.bipm.org)

[8] Petit G and Jiang Z 2008 GPS All in View time transfer for TAI computation *Metrologia* **45** 35-45

[9] Kirchner D, Ressler H, Hetzel P, Söring A and Lewandowski W 1999 Calibration of Three European TWSTFT Stations Using a Portable Station and Comparison of TWSTFT and GPS Common-View Measurement Results *Proc.*

30th Annual Precise Time and Time Interval (PTTI) Systems & Applications Meeting (Reston, VA, USA, 1998) pp 365-376

[10] Fujieda M, Aida M, Maeno H, Tung L Q and Amagai J 2007 Delay Difference Calibration of TWSTFT Earth Station Using Multichannel Modem *IEEE Trans. Instr. Meas.* **56** 346-350

[11] Matsakis D 2003 Time and Frequency Activities at the U.S. Naval Observatory *Proc. 34th Annual Precise Time and Time Interval (PTTI) Systems & Applications Meeting (Reston, VA,USA, 2002)* pp 437-456

[12] Breakiron L, Smith A, Fonville B, Powers E and Matsakis D 2005 The Accuracy of Two-Way Satellite Time Transfer Calibrations *Proc. 36th Annual Precise Time and Time Interval (PTTI) Systems & Applications Meeting (Washington, DC, USA, 2004)* pp 139-148

[13] Piester D, Bauch A, Becker J, Polewka T, McKinley A and Matsakis D 2004 Time Transfer between USNO and PTB: Operation and Calibration Results *Proc. 35th Annual Precise Time and Time Interval (PTTI) Systems & Applications Meeting (San Diego, CA, USA, 2003)* pp 93-101

[14] Piester D, Bauch A, Becker J, Polewka T, McKinley A, Breakiron L, Smith A, Fonville B and Matsakis D 2005 Two-Way Satellite Time Transfer between USNO and PTB *Proc. 2005 Joint IEEE Int. Freq. Contr. Symp. and Precise Time and Time Interval (PTTI) Systems & Applications Meetin*g *(Vancouver, Canada)* pp 316-323

[15] Piester D, Bauch A, Becker J, Polewka T, Rost M, Sibold D and Staliuniene E 2007 PTB's Time and Frequency Activities in 2006: New DCF77 Electronics, New NTP Servers, and Calibration Activities *Proc. 38th Annual Precise Time*

and Time Interval (PTTI) Systems & Applications Meeting (Reston, VA, USA, 2006) pp 37-47

[16] Cordara F, Lorini L, Pettiti V, Tavella P, Piester D, Becker J, Polewka T, de Jong G, Koudelka O, Ressler H, Blanzano B and Karel C 2004 Calibration of the IEN-PTB TWSTFT link with a portable reference station *Proc. 18th European Frequency and Time Forum (Guildford, UK)* on CD-ROM paper 137 pp 1-6

[17] Piester D, Hlaváč R, Achkar J, de Jong G, Blanzano B, Ressler H, Becker J, Merck P and Koudelka O 2005 Calibration of Four European TWSTFT Earth Stations with a Portable Station Through Intelsat 903 *Proc. 19th European Frequency and Time Forum (Besançon, France)* pp 354-359

[18] Piester D, Achkar J, Becker J, Blanzano B, Jaldehag K, de Jong G, Koudelka O, Lorini L, Ressler H, Rost M, Sesia I and Whibberley P 2006 Calibration of Six European TWSTFT Earth Stations Using a Portable Station *Proc. 20th European Frequency and Time Forum (Braunschweig, Germany)* pp 460-466

[19] Schlunegger C, Dudle G, Bernier L-G, Piester D, Becker J and Blanzano B 2007 Description of the TWSTFT Station at METAS and Presentation of the Calibration Campaign 2006 *Proc. IEEE Int. Frequency Control Symposium Jointly with 21st European Frequency and Time Forum (Geneva, Switzerland, 2007)* pp 918-922

[20] ITU Radiocommunication Sector 2003 The operational use of two-way satellite time and frequency transfer employing PN codes *Recommendation ITU-R TF.1153-2 (Geneva, Switzerland)*

[21] Post E J 1967 Sagnac Effect *Rev. Mod. Phys.* **39** 475-493

[22] Detoma E and Leschiutta S 1980 The Sirio-1 Timing Experiment *Proc. 11th Annual Precise Time and Time Interval (PTTI) Systems & Applications Meeting (Greenbelt, MD, USA, 1979)* pp 521-556

[23] de Jong G and Polderman M C 1995 Automated Delay Measurement System for an Earth Station for Two-Way Satellite Time and Frequency Transfer *Proc. 26th Annual Precise Time and Time Interval (PTTI) Systems & Applications Meeting (Reston, VA, USA, 1994)* pp 305-332

[24] Merck P and Achkar J 2005 Design of a Ku Band Delay Difference Calibration Device for TWSTFT Station *IEEE Trans. Inst. Meas.* **54** 814-818

[25] Matsakis D, Arias F, Bauch A, Davis J, Gotoh T, Hosokawa M, Piester D 2006 On Optimizing the Configuration of Time-Transfer Links Used to Generate TAI *Proc. 20th European Frequency and Time Forum (Braunschweig, Germany)* pp 448-454

[26] Takahashi Y, Fujieda M, Tung L Q, Tabuchi R, Nakagawa F, Maeno H, Aida M and Suzuyama T 2004 TWSTFT Network Status and Plans in the Pacific-Rim Region *Proc. Asia-Pacific Workshop on Time and Frequency 2004 (Beijing, China)* pp 250-257

[27] Hartl P, Gieschen N, Müssener K-M, Schäfer W and Wende C-M 1983 High accuracy global time transfer via geosynchronous telecommunication satellites with Mitrex *Z. Flugwiss. Weltraumforsch.* **7** 335-342

[28] Manufactured by Time Tech GmbH *(Stuttgart, Germany)*

[29] Powers E and Hahn J 2007 A report on GPS and Galileo Time Offset Coordination Efforts *Proc. IEEE Int. Frequency Control Symposium Jointly with 21st European Frequency and Time Forum (Geneva, Switzerland)* pp 440-445

[30] Ascarrunz F G, Jefferts S R and Parker T E 1997 Earth Station Errors in Two-Way Time and Frequency Transfer *IEEE Trans. Instr. Meas.* **46** 205-208

[31] Piester D, Bauch A, Becker J, Staliuniene E and Schlunegger C 2007 Studies on Measurement Noise in the European TWSTFT Network *Proc. 21st European Frequency and Time Forum (Geneva, Switzerland, 2007)* pp 1194-1199

[32] Fujieda M, Gotoh T, Aida M, Amagai J, Maeno H, Piester D, Bauch A and Yang S H 2007 Long Baseline TWSTFT Between Asia and Europe *Proc. 38th Annual Precise Time and Time Interval (PTTI) Systems and Applications Meeting (Reston, VA, USA, 2006)* pp 499-510

[33] Jiang Z, Dach R, Petit G, Schildknecht T and Hugentobler U 2006 Comparison and Combination of TAI Time links with continuous GPS Carrier Phase Results *Proc. 20th European Frequency and Time Forum (Braunschweig, Germany, 2006)* pp 440-447

[34] Hackman C, Levine J and Parker T E 2007 A Long-Term Comparison of GPS Carrier-Phase Frequency Transfer and Two-Way Satellite Time/Frequency Transfer *Proc. 38th Annual Precise Time and Time Interval (PTTI) Systems and Applications Meeting (Reston, VA, USA, 2006)* pp 485-498

[35] Bauch A, Piester D, Moudrak A and Petit G 2004 Time Comparison between USNO and PTB: A model for the determination of the time offset between GPS time and the future Galileo system time *Proc. 2004 IEEE International Ultrasonics, Ferroelectrics, and Frequency Control 50th Anniversary Joint Conference (Montréal, Canada)* pp 334-340

[36] Davis J A 1995 Theoretical Treatment of Closing Errors Occurring in Two-Way Satellite Time Transfer *Proc. 9th European Frequency and Time Forum (Besançon, France, 1995)* pp 537-540

[37] Davis J A, Pearce P R, Bartle K A, Hetzel P, Kirchner D, Ressler H, Powell W, McKinley A, De Young J A, Klepczynski W, de Jong G, Söring A, Baumont F, Claudon P, Grudler P, Hackman C and Veenstra L 1995 Closing Errors Observed During Two-Way Time Transfer Experiments *Proc. of 9th European Frequency and Time Forum (Besançon, France, 1995)* pp 81-86

[38] URL: ftp://ftp.bipm.org/TimeLink/LkC/, see the Readme file for explanations